

## Study of plasmoid drifts in massive material injection with JOREK

M. Kong<sup>1</sup>, E. Nardon<sup>2</sup>, D. Bonfiglio<sup>3</sup>, M. Hoelzl<sup>4</sup>, D. Hu<sup>5</sup>, the JOREK team\*

and the EUROfusion Tokamak Exploitation Team<sup>†</sup>

<sup>1</sup> *École Polytechnique Fédérale de Lausanne (EPFL), Swiss Plasma Center (SPC), CH-1015 Lausanne, Switzerland*

<sup>2</sup> *CEA, IRFM, F-13108 Saint-Paul-lez-Durance, France*

<sup>3</sup> *Consorzio RFX, Corso Stati Uniti 4, 35127 Padova, Italy*

<sup>4</sup> *Max Planck Institute for Plasma Physics, Boltzmannstr. 2, 85748 Garching b. M., Germany*

<sup>5</sup> *School of Physics, Beihang University, Beijing, 100191, China*

### Introduction

Ablation of cryogenic pellets in tokamak plasmas generates high density plasmoids. It is well known from hydrogen isotope pellet fuelling experiments that the ablation plasmoid moves towards the tokamak low field side (LFS) due to the  $\mathbf{E} \times \mathbf{B}$  drift originating from the polarization induced by  $\nabla B$  drift [1], where  $\mathbf{E}$  and  $\mathbf{B}$  are the electric and magnetic field, respectively. Recent 3D MHD modelling of deuterium ( $D_2$ ) shattered pellet injection (SPI) on JET have demonstrated that plasmoid drifts could also affect the effectiveness of runaway electron avoidance with LFS  $D_2$  SPI [2]. Even though 3D MHD codes like JOREK contain relevant physics, limitations on their toroidal resolution make it challenging to quantitatively resolve experimentally relevant plasmoids, e.g., those from SPI. To investigate this size effect and clarify plasmoid drifts in the presence of massive material injection (MMI), we present 3D JOREK simulations with a transient source deposited at the LFS midplane of a JET H-mode plasma (#96874).

### Plasmoid drift theory and simulation setup

In addition to the polarization current, the propagation of shear Alfvén waves (SAWs) from both ends of the plasmoid where different charges accumulate [3, 4] and the development of external parallel resistive currents connecting the top and bottom of the plasmoid [5] also contribute to limiting charge separation and thus plasmoid drifts, referred to as SAW braking and Pégourié braking, respectively. The latter occurs on a longer time scale and is strongly related to the toroidal extent of the source as it affects the external plasmoid-plasmoid connection length ( $L_{\text{con}}$ ). The drift velocity ( $V_D$ ) can be evaluated based on the zero divergence of current [3–6]. In particular, the early acceleration of plasmoid drifts when the SAW braking dominates was derived in a slab geometry and given in Eq. (1) [5], where the second term on the RHS represents SAW braking.  $p_0$  and  $p_\infty$  are the total plasmoid and background plasma pressure, respectively,

\*See the author list of M. Hoelzl et al. Nucl. Fusion (accepted) Doi: 10.1088/1741-4326/ad5a21

<sup>†</sup>See the author list of “Progress on an exhaust solution for a reactor using EUROfusion multi-machines capabilities” by E. Joffrin et al. to be published in Nuclear Fusion Special Issue: Overview and Summary Papers from the 29th Fusion Energy Conference (London, UK, 16-21 October 2023)

$n_0 = n_e$  is the plasmoid electron density,  $m_i$  the ion mass,  $Z_0$  the half-length of the plasmoid along the magnetic field line and  $C_A \equiv B/\sqrt{\mu_0 n_\infty m_i}$  the Alfvén speed, where  $n_\infty$  is the background electron density.

$$\dot{V}_D = \frac{2(p_0 - p_\infty)}{n_0 m_i R} - V_D \frac{2B_\phi^2}{\mu_0 C_A n_0 m_i Z_0}, \quad (1)$$

Considering  $p_0 \gg p_\infty$  and  $p_0 \equiv 2eT_e n_e$ , one can estimate the saturated drift velocity caused by the SAW braking below, where  $T_e$  is the plasmoid temperature in eV and  $e$  the electron charge.

$$V_{D,\text{lim}} \approx \frac{\mu_0 C_A p_0 Z_0}{R B_\phi^2} = \frac{2\mu_0 C_A e T_e n_e Z_0}{R B_\phi^2}. \quad (2)$$

The JOREK model used [7], initial equilibrium, computational grids and transport coefficients remain the same as Ref. [2]. The neutral source is deposited at  $R = 3.482$  m on the LFS midplane and with a Gaussian shape in toroidal, poloidal and radial directions, the half  $e^{-1}$  widths of which are denoted as  $\Delta\phi$ ,  $L_\theta$  and  $\Delta r$ , respectively.

### Effects of source amplitude

Deuterium neutrals are injected at a rate ranging from  $2 \times 10^{26}$  to  $1 \times 10^{28}$  atoms per second and for  $0.05 \mu\text{s}$ , with fixed  $\Delta\phi = 0.5$  and  $\Delta r = 4$  cm. Quantities evaluated at the source center are depicted in Fig. 1, where  $t = 0$  denotes the time when the neutral source starts. Given the large parallel

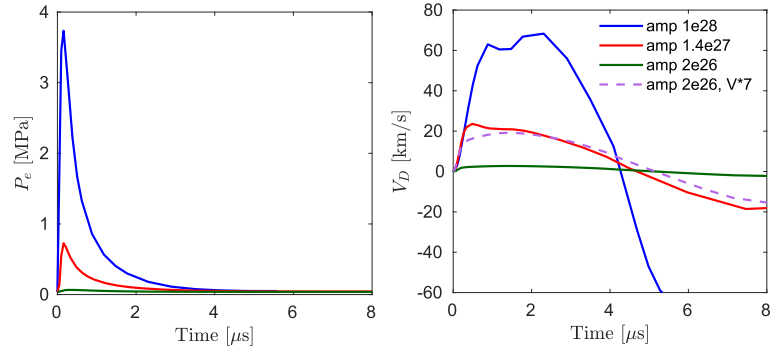


Figure 1: Time-evolution of  $p_e$  and  $V_D$  evaluated at the neutral source center with different injection rates marked in the legend. The source starts at  $t = 0$  and is cut off at  $0.05 \mu\text{s}$ .

heat conductivity, the local  $T_e$  equilibrates rapidly with the background plasma and remains around  $3.3$  keV.  $V_D$  initially increases due to the imbalanced pressure and quickly saturates via the braking effects. The main braking mechanism at play can be inferred by the dependence of  $V_{D,\text{lim}}$  on the source amplitude, which according to Eq. (2) has a linear dependence when the SAW braking dominates. As shown by the dashed purple line in Fig. 1,  $V_D$  of the amp– $2e26$  case matches well with that of the amp– $1.4e27$  case when scaling it by a factor of 7. This implies that the SAW braking dominates in cases with relatively small source amplitude.  $V_{D,\text{lim}}$  of the amp– $1e28$  case, however, is much lower than that from scaling its  $V_D$  based on the source amplitude. This can be explained by stronger Pégourié braking with larger source amplitude, which has stronger stochasticization that allows more efficient development of 3D parallel currents.

### Effects of source toroidal extent $\Delta\phi$

We focus on the amp–1.4e27 case here and vary  $\Delta\phi$  from 0.5 to 2 with fixed  $\Delta r = 4$  cm to study its effect on drifts. As illustrated by the dashed purple curve in Fig. 2, there is an earlier fast drop of  $V_D$  with larger  $\Delta\phi$ . This can be explained by the earlier onset of the Pégourié braking with larger  $\Delta\phi$  and thus lower  $L_{\text{con}}$ , as expected from theory [5]. In the rest of the paper we will focus on cases with  $\Delta\phi = 0.5$  and relatively small source amplitude to study the effects of the SAW braking on plasmoid drifts and aim at a quantitative comparison with theory.

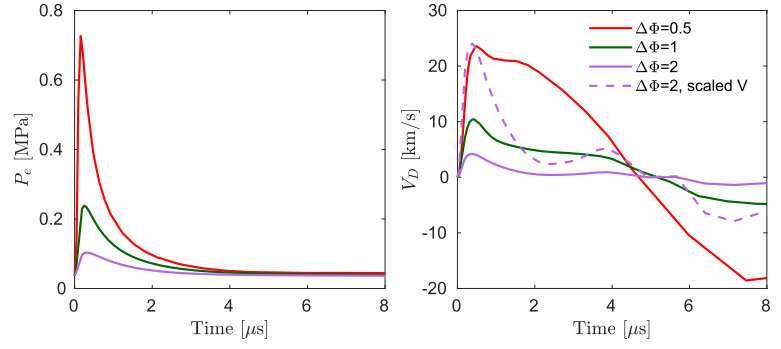


Figure 2: Time-evolution of  $p_e$  and  $V_D$  evaluated at the source center with different  $\Delta\phi$ . The dashed purple curve is a scaling (by a factor of 5.7) of the solid purple case to help guide the eyes.

### Comparison with plasmoid drift theory

We estimate  $V_{D,\text{lim}}$  with Eq. (2) and compare with those obtained from JOREK simulations.  $2n_e Z_0$  is effectively the line-integrated plasmoid density along a magnetic field line and varies insubstantially after ionization. This facilitates evaluating  $V_{D,\text{lim}}$  for cases where the SAW braking dominates. The amp–1.4e27 case shown by the red curves in Figs. 1 and 2, for example, has  $V_{D,\text{lim}} \approx 75$  km/s based on Eq. (2), which is 3.75 times those obtained from simulations shown in the figures ( $\sim 20$  km/s). Similar phenomenon has been observed for cases with lower source amplitude, though not shown here for conciseness. A possible explanation is that Eq. (2) only considers magnetic field lines passing through the source region, whereas in reality more field lines are bent, causing stronger SAW braking. This is reflected by the near circular flow region on the poloidal plane as  $\mathbf{E}$  is a dipole field, whereas the plasmoid is more poloidally elongated than radially (Fig. 3). A possibly more appropriate way of applying Eq. (2) in 3D MHD simulations is using an averaged  $p_e$  over the  $\mathbf{E} \times \mathbf{B}$  flow region. As a crude estimation, we track about 1600 magnetic field lines originating from the flow region marked by the rectangle in Fig. 3. The average line-integrated plasmoid pressure is only about 1/3.6 of that passing through the source region, explaining well the discrepancy above.

### Effects of the size of the $\mathbf{E} \times \mathbf{B}$ flow region

$n_e$  and the  $\mathbf{E} \times \mathbf{B}$  flow potential ( $U$ ) on the injection plane of two cases with the same  $\Delta\phi = 0.5$  but  $\Delta r = 4$  cm and 8 cm, respectively, are shown in Fig. 3, exhibiting similar  $\mathbf{E} \times \mathbf{B}$  flow region. This as expected since  $\Delta r \ll R\Delta\phi B_\theta/B_\phi = L_\theta$  here, i.e. the size of the  $\mathbf{E} \times \mathbf{B}$  flow region on the poloidal plane depends on the poloidal size and thus the toroidal size of the plasmoid, where

$B_\theta$  is the poloidal magnetic field. As a result,  $V_D$  is very similar in these two cases despite very different local  $n_e$  and  $p_e$  (not shown here for conciseness), emphasizing the important role of the  $\mathbf{E} \times \mathbf{B}$  flow region in plasmoid drifts.

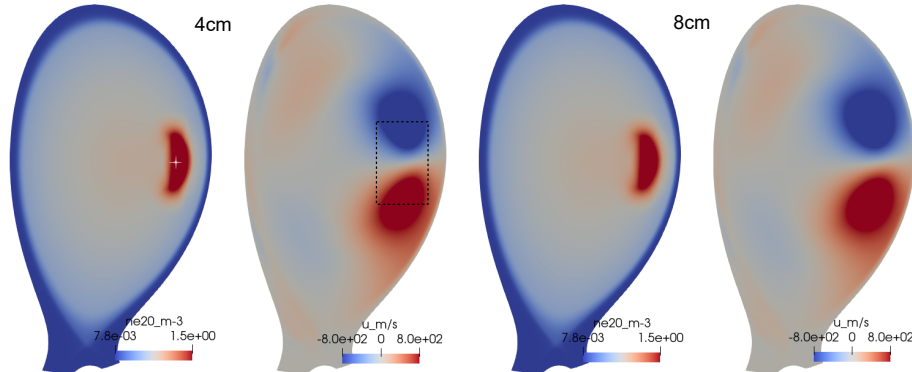


Figure 3:  $n_e$  and  $U$  with  $\Delta r = 4$  cm and  $8$  cm, respectively. The white cross marks the source center.

### Conclusions and outlook

Plasmoid drifts in the presence of MMI have been studied via 3D MHD modelling with JOREK, using a transient neutral source deposited at the LFS midplane of a JET H-mode plasma. The simulations have reached good agreement with existing theory. For instance, the drift velocity is limited by SAW braking for cases with small source amplitude and Pégourié braking sets in earlier with larger toroidal source extent. Pégourié braking has been found to be stronger with larger source amplitude, probably due to earlier and stronger stochasticization that allows more efficient mixing of field lines and development of parallel resistive currents. The simulations have also identified the key role of the size of the  $\mathbf{E} \times \mathbf{B}$  flow region on plasmoid drifts and showed that  $V_{D,\text{lim}}$  from simulations matches with theory when considering an effective pressure within the flow region. Effects of including a small percentage of neon in the neutral source and using multiple sources will be explored in the future, in view of SPI studies.

*This work has been carried out within the framework of the EUROfusion Consortium, funded by the European Union via the Euratom Research and Training Programme (Grant Agreement No 101052200 — EUROfusion). The Swiss contribution to this work has been funded by the Swiss State Secretariat for Education, Research and Innovation (SERI). Views and opinions expressed are however those of the author(s) only and do not necessarily reflect those of the European Union, the European Commission or the SERI. Neither the European Union nor the European Commission nor SERI can be held responsible for them. This work was supported in part by the Swiss National Science Foundation. This work is summarized based on results from “M. Kong et al., 3D MHD modelling of plasmoid drift following massive material injection in a tokamak, Nucl. Fusion (to be submitted), preprint at [arxiv.org/abs/2407.01399](https://arxiv.org/abs/2407.01399)”.*

### References

- |   |   |
|---|---|
| [1] H.W. Müller, et al, Nucl. Fusion <b>42</b> , 301 (2002) | [4] V. Rozhansky et al, PPCF <b>46</b> , 575 (2004)       |
| [2] M. Kong et al, Nucl. Fusion <b>64</b> , 066004 (2024)   | [5] B. Pégourié et al, Nucl. Fusion <b>47</b> , 44 (2007) |
| [3] P.B. Parks et al, Phys. Plasmas <b>7</b> , 1968 (2000)  | [6] O. Vallhagen et al, JPP <b>89</b> , 905890306 (2023)  |
|   | [7] M. Hoelzl et al. Nucl. Fusion <b>61</b> 065001 (2021) |